Ex vivo characterization of sub-10-fs pulses

Adam M. Larson and Alvin T. Yeh

Department of Biomedical Engineering, Texas A&M University, 337 Zachry Engineering Center, 3120 TAMU, College Station, Texas 77843

Received January 13, 2006; revised March 7, 2006; accepted March 20, 2006; posted March 22, 2006 (Doc. ID 67240)

An all-mirror dispersion-compensation setup is used to correct for quadratic and cubic phase distortions induced within a custom nonlinear optical microscope. Mouse tail tendon is used to characterize sub-10-fs pulses by interferometric autocorrelation. This is an ideal method for characterizing dispersion from the optical system, immersion medium, and wet biological sample. The generation of very short autocorrelations demonstrates the ability to compensate for phase distortions within the imaging system and efficient second-harmonic upconversion of the ultrashort pulse spectrum within collagen. Compensated autocorrelation traces are presented for biologically relevant objective lenses. © 2006 Optical Society of America

OCIS codes: 170.7160, 110.0180, 320.0320, 170.6930.

Nonlinear optical microscopy (NLOM) utilizes optical signals resulting from nonlinear laser–tissue interactions for imaging and spectroscopy. High peak intensities provided by ultrafast laser pulses focused through high numerical aperture (NA) objectives can generate observable nonlinear optical signals [e.g., two-photon excited fluorescence[1] or second-harmonic generation[2] (SHG)] with low average input powers. The nonlinear dependence of these optical signals on laser intensity facilitates optical sectioning, rendering thin images from within thick specimens and alleviating the need for destructive sample processing (i.e., fixing, sectioning, staining). These attributes are conducive for serial measurements that can follow the progression of biological processes in a single experimental tissue sample.

Temporally shorter laser pulses have higher peak intensities with minimal average input powers, making nonlinear optical signals accessible from exogenous markers or endogenous biological constituents with low nonlinear susceptibilities while minimizing sample damage. Shorter pulses necessarily have broader bandwidths; sub-10-fs pulses used in our custom-built NLOM system have spectra centered at 800 nm with a full width at half-maximum (FWHM) of 133 nm (see Fig. 1B).

Laser pulses of ultrashort duration are highly susceptible to phase distortions introduced by the NLOM optical system, particularly through the use of high NA objectives.[3–7] Delivery of sub-10-fs pulses to the specimen requires minimization of (or compensation for) phase distortions introduced by the NLOM optical system. Compression of 6 fs pulses was demonstrated by compensating for quadratic [group delay dispersion (GDD)] and cubic [third-order dispersion (TOD)] phase distortion using a grating and prism sequence.[8] Previous works have examined the effects of ultrashort pulse propagation (ranging from 170 to 15 fs[5,6,9,10]) in NLOM optical systems and minimized phase distortions at the focal plane using prisms. In contrast to a prism and grating sequence where overall negative GDD and TOD are a function of prism material and interelement spacing, dispersion-compensating mirrors (DCMs) induce a fixed amount of linear negative chirp with each reflection. This allows compact, high throughput compensation configurations with less sensitivity to optical alignment. In this Letter, we demonstrate minimization of phase distortions in sub-10-fs pulses at the focus of a custom-built NLOM system using a DCM.

The interferometric autocorrelation (inset, Fig. 1A) and spectrum (Fig. 1B) are shown for sub-10-fs pulses from a Kerr-lens mode-locked $Ti:Al_2O_3$ oscillator (Femtosource Compact, Femtolasers) pumped by a frequency-doubled $Nd:YVO_4$ solid-state laser (Verdi, Coherent). With 4.0 W of pump power, 7 nJ pulses are achieved at 75 MHz and directed to dispersion control optics consisting of a DCM[11] (GSM210, Femtolasers), antireflection-coated windows, and a fused silica wedge pair (OA124, Femtolasers). A planoconvex lens ($f=1000$ mm, $d=25.4$ mm) is placed after the oscillator to control beam divergence of the laser through the NLOM optical system. A half-wave plate and polarizer are used for controlled attenuation of laser intensity.

The double-pass configuration of the DCM allows a total of 32 bounces. This geometry gives simple dispersion tuning of up to -6400 fs^2 and -3840 fs^3 in increments of -400 fs^2 and -240 fs^3 in GDD and TOD, respectively, at 800 nm with 82% (94% if retroreflector losses are neglected) efficiency after 16 bounces. The fixed negative chirp imparted by the DCM per reflection requires the addition of glass to the beam path for fine dispersion-compensation adjustments. We use combinations of antireflection-coated BK7 windows at 2, 3, or 4 mm thickness and fused silica

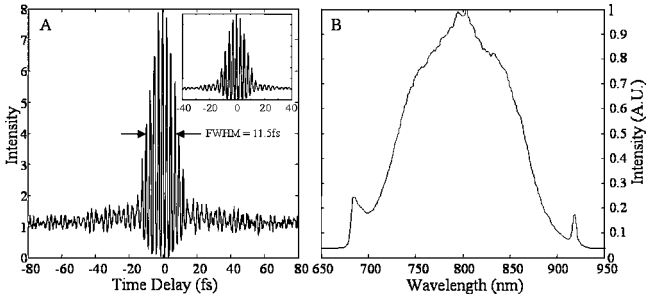

Fig. 1. Interferometric autocorrelation of a sub-10-fs laser pulse (inset, from an oscillator) A, after propagation through a 20× Plan-Apochromat, 0.75 NA objective; B, spectrum measuring 133 nm FWHM centered at 800 nm.

0146-9592/06/111681-3/$15.00

wedge pair, each mounted on a linear translation stage providing an additional 400 μm to 3 mm of glass. This corresponds to precise control of up to 518.2 fs^2 GDD and 62.5 fs^3 TOD.

The laser is coupled into the epifluorescence port of an upright microscope (Axioskop2 MAT, Zeiss) via dual-axis galvanometer driven mirrors (Cambridge Technology) mounted on an elevated breadboard and controlled by commercially available software and a three-axis control board (Vista, ISS). A 1.5:1 beam-expanding telescope comprised of two near-IR designed achromatic lenses appropriately images a spot from between the galvanometer mirrors to the back focal aperture (BFA) of the microscope objective. It has been reported[3] and experimentally shown[12] that significant pulse broadening can occur because of nonconstant GDD across the face of a lens, leading to a propagation time difference (PTD). PTD results in a nonconstant distortion between the pulse front and the phase front, and, consequently, overcompensation for dispersion in pulses traveling closer to the marginal ray. To minimize this effect, near-IR achromatic lenses have been used in the beam expander.

The beam is directed to the microscope objective by a short-pass dichroic mirror (635dcspxruv3p, Chroma). Nonlinear optical signals are collected by the focusing objective and directed to a two-channel detector unit mounted on an accessory port of the binocular head. The detector unit houses dichroic mirrors, bandpass filters (Chroma), focusing lenses, and a pair of photon-counting photomultiplier tubes (PMTs; R7400P, Hamamatsu). In imaging mode each PMT is connected to a preamplifier/discriminator (F100T, Advanced Research Instruments) that feeds a counter managed by software. Image intensities are displayed in counts per second on a PC.

For pulse width measurements, a low-dispersion interferometric autocorrelator (Femtometer, Femtolasers) is inserted into the optical path with its curved mirror removed to allow collinear beams to be directed to the microscope. Typically, water-immersion objectives are used for biological imaging applications. Consequently, characterization of dispersion in a NLOM optical system should account for the immersion medium. For example, a water-immersion objective with a 3.6 mm working distance corresponds to 88.7 fs^2 and 18.4 fs^3 of GDD and TOD, respectively, as calculated from the refractive index of water,[13] corresponding to a broadening factor of $\sim$7.

Mouse tail tendon (MTT) immersed in phosphate-buffered saline was used to generate a second-order (SHG) interferometric autocorrelation signal. A representative image of MTT when SHG in collagen was used, was obtained with a 63$\times$ Achroplan, 0.95 NA (Zeiss) objective (inset, Fig. 2D). Backscattered laser light was filtered during autocorrelation measurements using 1 mm of BG-39 Schott glass filter.

The autocorrelation traces in Fig. 2 show distinctive sidelobes on either side of the central peak. The FWHM of the central peak is reported as minimum pulse width (see Table 1). The sidelobes are the result of cross correlation between a broadened, marginal

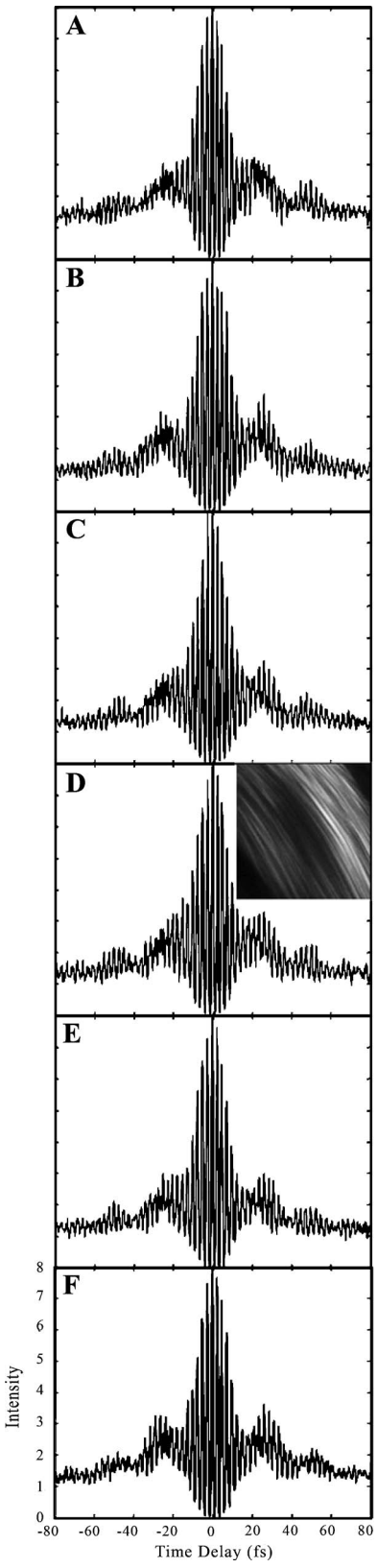

Fig. 2. Interferometric autocorrelation at the NLOM focal plane using A, 20$\times$ Plan-Apochromat, 0.75 NA; B, 20$\times$ Achroplan, 0.5 NA; C, 40$\times$ Achroplan, 0.8 NA; D, 63$\times$ Achroplan, 0.95 NA; E, 100$\times$ Achroplan, 1.0 NA; and F, 63$\times$ C-Apochromat, 1.2 NA. A representative image of mouse tail tendon is shown in the inset of D.

Table 1. Calculated Dispersion Parameters, Minimum Pulse Width (±0.4 fs), D_r, and Total Delay (±2.7 fs) of the Pulse

Component	GVD (fs^2)	TOD (fs^3)	Minumum Pulse Width (fs)	D_r	Total Delay (fs)
20× Achroplan 0.5 NA	−3818.7	−2378.4	12.5	1.0	26.5
40× Achroplan 0.8 NA	−4000.0	−2400.0	12.7	0.7	25.4
63× Achroplan 0.95 NA	−3728.0	−2367.6	12.3	1.0	26.5
100× Achroplan 1.0 NA	−3464.0	−2143.8	11.3	1.4	26.5
20×Plan-Apochromat 0.75 NA	−3728.0	−2367.6	11.7	0.7	21.1
63× C-Apochromat 1.2 NA	−4528.0	−2847.6	11.9	1.2	25.1

ray and an optimally compensated pulse traveling along the optical axis at the paraxial focus.[7] Delay between the central and the sidelobe peaks is associated with chromatic and spherical aberration within the optical system.[14] This is reported as total delay in Table 1 and indicates the delay for pulses passing radially through the system. The values of total delay are consistent with previously reported studies.[7]

With the curved mirror in place, the interferometric autocorrelation in Fig. 1A, obtained using a 20× Plan-Apochromat, 0.75 NA (Zeiss) air objective collimated by a near-IR achromat outside the microscope, does not show sidelobes because the beam diameter relative to the BFA was $D_r = 0.32$. The FWHM of 11.5 fs compared with 11.7 fs for the identical objective using MTT at $D_r = 0.7$ (Fig. 2A) justifies our minimum pulse width. The effects of spherical and chromatic aberration can be minimized for $D_r < 0.4$, allowing one to obtain the original pulse width.[7] With $D_r > 0.4$, aberration increases quadratically with radial distance. The actual pulse width of a 10 fs laser has been measured at the paraxial focus of a singlet lens with chromatic and spherical aberrations.[4] Furthermore, such aberrations are responsible for distortions in the spatial field at the focus.[15]

The Achroplan series of objectives all share similar spherical and chromatic aberration. The 20× Plan-Apochromat shows the least amount of total delay with a minimum objective contribution to aberration while realizing the full aberration induced by the telescope. The 63× C-Apochromat, 1.2 NA, shows the shortest total delay, with an overfilled aperture indicating its higher level of aberration correction. Aside from the 100× Achroplan, 1.0 NA, the two most well-corrected objectives yield the shortest minimum pulse width. The 100× Achroplan yields shortest pulse widths because it has the least dispersion to compensate for and, thus, the smallest residual TOD. Pulse width calculations, optic dispersion parameters, and D_r for each objective are presented in Table 1.

We have demonstrated the ability to compensate for phase distortions induced by ultrashort pulse propagation through a complete NLOM optical system. To our knowledge, this is the first time aberration and dispersion have been characterized in a NLOM optical system using sub-10-fs pulses. The ability to obtain minimally broadened pulses within a MTT preparation indicates that nearly the entire pulse spectrum is being upconverted and the phase-matching condition is significantly relaxed. New capabilities may be realized with NLOM utilizing dispersion-compensated ultrashort pulses, including efficient, simultaneous excitation of multiple fluorophores and laser microsurgery[16,17] without pulse amplification.

We thank Gabriel Tempea of Femtolasers Produktions for technical discussions. Funding was provided by the National Science Foundation Faculty Early Career Development (CAREER) Award and by the National Institutes of Health (R21 EB004846-01).
A. Yeh's e-mail address is ayeh@tamu.edu.

References

1. W. R. Zipfel, R. M. Williams, and W. W. Webb, Nat. Biotechnol. **21**, 1369 (2003).
2. P. J. Campagnola and L. M. Loew, Nat. Biotechnol. **21**, 1356 (2003).
3. Z. Bor, Opt. Lett. **14**, 119 (1989).
4. M. Kempe and W. Rudolph, Opt. Lett. **18**, 137 (1993).
5. J. B. Guild, C. Xu, and W. W. Webb, Appl. Opt. **36**, 397 (1997).
6. M. Muller, J. Squier, R. Wolleschensky, U. Simon, and G. J. Brakenhoff, J. Microsc. **191**, 141 (1998).
7. J. Jasapara and W. Rudolph, Opt. Lett. **24**, 777 (1999).
8. R. L. Fork, C. H. B. Cruz, P. C. Becker, and C. V. Shank, Opt. Lett. **12**, 483 (1987).
9. G. J. Brakenhoff, M. Muller, and J. Squier, J. Microsc. **179**, 253 (1995).
10. V. Iyer, B. E. Losavio, and P. Saggau, J. Biomed. Opt. **8**, 460 (2003).
11. P. Dombi, V. S. Yakovlev, K. O'Keeffe, T. Fuji, M. Lezius, and G. Tempea, Opt. Express **13**, 10888 (2005).
12. T. A. Planchon, S. Ferre, G. Hamoniaux, G. Cheriaux, and J.-P. Chambaret, Opt. Lett. **29**, 2300 (2004).
13. A. G. Van Engen, S. A. Diddams, and T. S. Clement, Appl. Opt. **37**, 5679 (1998).
14. M. Kempe and W. Rudolph, Phys. Rev. A **48**, 4721 (1993).
15. M. Kempe, U. Stamm, B. Wilhelmi, and W. Rudolph, J. Opt. Soc. Am. B **9**, 1158 (1992).
16. M. F. Yanik, H. Cinar, H. N. Cinar, A. D. Chisholm, Y. Jin, and A. Ben-Yakar, Nature **432**, 822 (2004).
17. I. Maxwell, S. Chung, and E. Mazur, Med. Laser. Appl. **20**, 193 (2005).